

Ethylene-Bridged Hexadentate Bis(amidines) and Bis(amidinates) with Variable Binding Sites

Connor O'Dea,[†] Omar Ugarte Trejo,[†] Janet Arras,[†] Andreas Ehnbom,[‡] Nattamai Bhuvanesh,[‡] and Michael Stollenz*^{,†}®

Supporting Information

ABSTRACT: Hexadentate bis(amidines) form versatile networks of hydrogen bonds both in solid state and solution, as revealed by X-ray crystallography, IR, and NMR spectroscopy. Moreover, the corresponding bis(amidinates) produce blue and green emissions in THF solution. Tethered tetradentate bis(amidines) have emerged in coordination chemistry, enantioselective catalysis, as building blocks for polyfunctional heterocycles, and in photoluminescent materials. The next generation of flexible bis(amidine)/bis(amidinate) platforms with up to six N-donor sites has now been established.

he great versatility of amidines and bis(amidines) has resulted in widespread applications as biochemical reagents of pharmaceutical interest, precursors for heterocycles serving as redox-switchable chromophores/fluorophores, and also as important ligands in coordination chemistry. 1-3 This is because of their isoelectronic relation to carboxylic acids and esters, although amidines are substantially more versatile than their oxygen congeners, due to the fact that a large variety of additional functional substituents and linking groups can be attached to the basic amidine moiety.

Since their seminal discovery in the early 1950s,4 alkylenebridged bis(amidines) have attracted considerable attention, primarily as striking analogues to tethered bis-(cyclopentadienyl) ligand scaffolds in "constrained" ansa metallocenes⁵ which have revolutionized homogeneous polymerization catalysis. In particular, bis(amidines) linked to alkylene and arylene backbones have emerged in lanthanide and in Group 4 complex chemistry, along with other related demanding catalytic applications, including asymmetric catalysis.^{3,6,7} These polydentate ligands have also been found to be suitable for embedding multinuclear transition-metal-ion assemblies. 6c,7b,e,f,j,8,9

We have recently reported on a new ethylene diamine-based bis(amidine) 1 with bulky terminal mesityl substituents that serves as a ligand of a rare luminescent homoleptic and tetranuclear Cu^I array. 10 This complex was obtained from 1 and mesitylcopper, a powerful synthon for multiple Cu^I scaffolds (Figure 1).11

Figure 1. New ethylene-bridged N,N'-disubstituted bis(amidines) 1-

Although related trans-1,2-diaminocyclohexane-linked tetradentate (t-1,2-DACH-)bis(amidines) and their corresponding alkali metal complexes have been in the focus of two earlier studies, significantly less attention has been devoted to bis(amidines) bearing additional terminal N-donor sites. 6a,b This is surprising, as these bis(amidines) are generally interesting in terms of their potential as hexadentate ligands and hydrogen bond donor-acceptor properties in feasible supramolecular assemblies. This becomes obvious when the large family of related nonaromatic 1,3,5-triazapentadienes and pentaazadienes, their less explored N-analogues, is considered. 12–15 In particular, 1,3,5-triazapentadiene anions have been employed as versatile ligands for Groups 1-2 and 7-13 element complexes as well as in accompanying catalytic

Received: July 18, 2019 Published: September 27, 2019

[†]Department of Chemistry and Biochemistry, Kennesaw State University, 370 Paulding Avenue NW, MD #1203, Kennesaw, Georgia 30144, United States

^{*}Department of Chemistry, Texas A&M University, 580 Ross Street, P.O. Box 30012, College Station, Texas 77842-3012, United States

applications. 13,14 The corresponding BF₂/BPh₂ complexes are of significant interest as highly luminescent materials. 12i,k Out of this selection, linked bis- and tris(1,3,5-triazapentadienes) have been described in the literature as well. 12g,h,j,k Among the less prominent linked (t-1,2-DACH-)bis(amidines), only one example with terminal pyridyl substituents has been reported so far. 6b Remarkably, closely related pyridylbenzamidines are well-known for decades and have recently attracted considerable attention as ligands in nickel- and palladium-catalyzed cross coupling reactions and in olefin polymerization/oligomerization. Only one example of a corresponding pyridyl(tert-butyl)amidine has been published so far. 17 In contrast to these potentially tridendate monoamidines bearing an additional pyridyl donor site, information on the molecular structures of linked hexadentate bis(amidines), both in solution and solid state, has remained fragmentary to date. Solid-state structures of hexadentate bis(amidines) have not been reported at all. Accompanying computational studies are entirely missing.

Herein, we report the synthesis and molecular structures of the new *N*,*N*′-disubstituted bis(amidines) **2–6**, some of which show a remarkable network of *inter*- and *intra*molecular NH··· N′ hydrogen bonds in the solid state (Figure 1). A comprehensive computational study (gas phase and solution) of **2–6** is provided as well. Moreover, we have discovered that **2–6** become highly emissive in THF solutions upon deprotonation through "BuLi or NaN(SiMe₃)₂. Thus, **2–6** and their dianions represent a series of unprecedented photoluminescent bis(amidine)/bis(amidinate) light switches.

The synthesis of 2-6 followed a straightforward three-step protocol that was accompanied by reasonable to good yields (54–63%, Scheme 1).

Scheme 1. Three-Step Synthesis of $2-6^a$

^aKey: **2**: R^1 , $R^2 = H$; **3**: $R^1 = Me$, $R^2 = H$; **4**: $R^1 = H$, $R^2 = Me$; **5**: R^1 , $R^2 = Me$; **6**: $R^1 = C_4H_4$, $R^2 = H$.

Bis(amide) **A** was easily obtained from ethylenediamine and 2 equiv of pivaloyl chloride in the presence of triethylamine, similarly to earlier reported procedures. Upon reaction with PCl_5 , the corresponding bis(imidoyl chloride) **B** was isolated as an air- and temperature-sensitive pale yellow oil. Exposure to room temperature for more than about 24 h resulted in decomposition that was indicated by an orange-brownish color change. Subsequent aminolysis and basic workup yielded the bis(amidines) 2-6 as colorless microcrystalline solids.

The 1 H NMR spectra of **2–6** (both recorded in CDCl₃ and in C_6D_6) show one set of sharp resonances for all C–H protons and therefore suggest the presence of one symmetrical stereoisomer in solution (see Table S6 and Figures S15–S34 in the Supporting Information). The bulky *tert*-butyl groups

produce sharp singlets between $\delta = 1.17$ and 1.32 ppm, thus indicating fast rotation. The molecular flexibility of 2-6 in solution is also confirmed by the CH₂ signals ($\delta = 3.01-3.20$ ppm) as no substantial line broadening is observed. This is in striking contrast to our previously reported bis(amidine) 1 that generally produces broad resonance signals in its C_6D_6 ¹H NMR spectrum at room temperature. ^{10,18} In addition, a series of even more broadened signals at $\delta = 3.02$, 5.72, and 7.89 ppm was found. These additional signals suggest that C=N doublebond stereoisomers (EE, EZ/ZE, and ZZ) and their syn/anti rotational isomers exist in solution that interconvert through tautomerism and C-N single-bond rotation at the amidine moieties. Overall, eight distinct and four additional pairs of identical stereoisomers are possible for ethylene-bridged N_iN' disubstituted bis(amidines), if the predominant tautomer retains the $-NH(CH_2)_2NH$ diamine core motif, which is confirmed for the solid state by the XRD structures of 1, 3, 5, and 6 (vide infra).

Substantial line broadening is only observed for the N-H resonances in the ¹H NMR C₆D₆ spectra of 2-6 when contrasted with the CDCl₃ data. This is most evident for 6 as the corresponding N-H signal in C_6D_6 is too broad to be detected at ambient temperature. All N-H resonances of 2-5 in C_6D_6 are remarkably downfield shifted ($|\Delta\delta| \approx 0.86-1.68$ ppm) relative to the sterically crowded bis(amidine) 1 (Table S6). Since the electronic effect of the more electronwithdrawing pyridyl and quinolyl substituents of 2-6 on the CH_2 proton shifts of the common $-NH(CH_2)_2NH$ linking core is less significant than on the N-H resonances ($|\Delta\delta| \approx$ 0.03-0.70 relative to 1), sole electronic effects of the terminal aryl substituents do not explain the magnitude of the N-H shifts. Instead, there is strong evidence for hydrogen bonding being present in solution for 2-6, which was confirmed for the solid state (vide infra) and supported by DFT calculations (Figure 2, Schemes S1 and S2, and Tables S7-S9). 19,20 The

$$R^{2}$$

$$R^{1}$$

$$R^{2}$$

$$R^{1}$$

$$R^{2}$$

$$R^{1}$$

$$R^{2}$$

$$R^{1}$$

$$R^{2}$$

$$R^{2}$$

$$R^{2}$$

$$R^{2}$$

$$R^{2}$$

$$R^{3}$$

$$R^{2}$$

$$R^{2}$$

$$R^{2}$$

$$R^{2}$$

$$R^{2}$$

$$R^{3}$$

$$R^{2}$$

$$R^{2}$$

$$R^{3}$$

$$R^{2}$$

$$R^{3}$$

$$R^{2}$$

$$R^{3}$$

$$R^{2}$$

$$R^{3}$$

$$R^{2}$$

$$R^{3}$$

$$R^{2}$$

$$R^{3}$$

$$R^{4}$$

$$R^{2}$$

$$R^{4}$$

$$R^{4}$$

$$R^{2}$$

$$R^{4}$$

$$R^{4}$$

$$R^{2}$$

$$R^{4}$$

$$R^{4}$$

$$R^{4}$$

$$R^{4}$$

$$R^{2}$$

$$R^{4}$$

$$R^{5}$$

$$R^{4}$$

$$R^{5}$$

$$R^{4}$$

$$R^{5}$$

$$R^{5$$

Figure 2. Calculated rotational isomers I-IV of 2-6.

deshielding effect of hydrogen bonds is more distinct in less polar C_6D_6 as $CDCl_3$ serves as a weak hydrogen bond donor/acceptor. In addition, variable-temperature 1H NMR spectra of **2–6** in THF- d_8 reveal a notable downfield-shift by up to 0.83 ppm from 27 $^{\circ}C$ to -100 $^{\circ}C$ (Figure S35–S39). These experimental observations are consistent with the calculated gas-phase structures **I–III** that all show intramolecular hydrogen bonding, thus suggesting *intra*molecular N–H···N

hydrogen bonds being present in solution for 2–6. In contrast, the two cases in which hydrogen bonding is absent (calculated 1 and IV) substantially upfield-shifted NH resonance signals were found (Scheme S2).

The 13 C 1 H 13 NMR spectra of **2–6** in CDCl 13 and C 6 D 6 are very similar and show the diagnostic peaks of the common -N=C $^{(1)}$ Bu 13 NH $^{(1)}$ CH 13 2NH $^{(1)}$ Bu 13 C=N 13 Core motif at δ = 29.2 13 29.5, 39.0 13 39.0 13 39.1, 43.4 13 43.5 (CH 13 2), and 162.5 13 164.6 ppm (amidine signal, Table S10). All peaks were completely assigned by a series of 2D NMR experiments (see the Experimental Section). Only for 4 and 5 in CDCl 13 3, the close proximity of the amidine carbon resonance to the pyridyl-C-2 signal frustrates an unambiguous assignment of both peaks.

Next, the solid-state structures of the hexadentate bis-(amidines) were examined. Single crystals of **3**, **5**·C₆D₆, and **6** were obtained from mixtures of THF/diethyl ether, $C_6D_6/$ hexanes, and $CH_2Cl_2/\text{diethyl}$ ether, respectively. X-ray crystallography reveals ZZ(syn/syn) stereoisomers of **3** and **6** being exclusively present in the crystal lattice whereas **5** features an EZ(syn/syn) isomeric configuration (Figure 3 and SI).²²

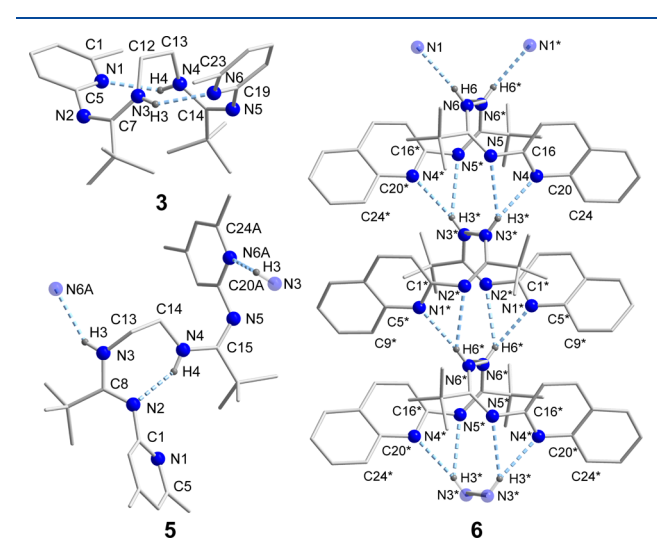


Figure 3. XRD molecular structures of 3, 5, and 6.23

As opposed to the sterically crowded bis(amidine) 1, its hexadentate congeners 3, 5, and 6 form a versatile network of intra- and intermolecular NH···N′ hydrogen bonds that are, according to Jeffery's classification, weak to moderately strong as evidenced by donor–acceptor distances of 2.93–3.35 Å, NH···N distances of 2.18–2.64 Å and N–H···N angles of $137-151^{\circ}$ (Table S4). ²⁴ This is consistent with the IR ν (N–H) stretching frequencies of 2–6 which are red-shifted by 95–152 cm⁻¹ relative to bis(amidine) 1 that does not show evidence of hydrogen bonding in the solid state (Table S5).

A common feature of all bis(amidine) structures 1-6 is that the N-H protons reside on the more basic N-donor sites of the central $-NH(CH_2)_2NH-$ diamine linker. The molecular structure of 3 reveals *two intra*molecular hydrogen bonds to the pyridyl N-donor sites serving as hydrogen-bond acceptors. This results in the formation of two nine-membered rings in the bis(amidine) framework with an overall C_2 symmetry of 3. Introducing additional methyl substituents in the 4-pyridyl positions (5) gives rise to *one intra*molecular hydrogen bridge with the amidine-N atom acting as hydrogen bond acceptor. As

a consequence, a seven-membered ring in the bis(amidine) moiety is formed. In addition, *inter*molecular hydrogen bonds to the pyridyl-N hydrogen bond acceptors of the next neighbored ligand molecules in the crystal lattice are observed, thus resulting in a polymeric chain of 5. Similar to 3, bis(amidine) 6 adopts C_2 symmetry, but in contrast, it shows exclusively *inter*molecular hydrogen bonding that originates from accepting two NH donors by the two quinolyl end groups of the next neighbored molecule to form 14-membered rings throughout the polymeric chain. There are no additional intermolecular contacts in the crystal packings of 3, $5 \cdot C_6 D_6$, and 6 (Figures S3, S6, and S10).

In consequence of the pronounced N–C single bond character of the central $-NH(CH_2)_2NH$ — diamine bridge, a large Δ_{CN} parameter²⁵ is observed for 1 (0.077) that indicates only a low extent of delocalization within the -N=C-N-moieties. Electron-deficient pyridyl and quinolyl substituents in 3, 5, and 6 result in smaller Δ_{CN} values (0.039–0.0624 Å) and thus increased delocalization which is most pronounced in 6 (Table S3).

E/Z isomerization tremendously impacts the N=C-NH angles of 1, 3, 5, and 6—they are significantly (up to about 12°) larger in ZZ isomers than in EE isomers, which is consistent with the increased steric constraints on the amidine moieties of the observed examples.

Remarkably, the XRD molecular structures of 3, 5, and 6 also represent the three lowest energy structures as predicted by density functional theory (DFT). We turned to computational tools to help us understand which rotational isomers could be accessible in solution and if the internal hydrogen bonding would give stability preferences for one species over another. The relative stability (kcal/mol) for selected rotamers of 2-6 (I-IV) was modeled both in the gas phase and in solvents of different polarity (C₆H₆ vs CHCl₃) using DFT at the B3LYP/6-311G(d) level (Schemes S3-S7). Rotamers I, II, and IV (that are consistent with the XRD structures of 3, 5, and 6, respectively) are all within the range of 3.9 kcal/mol (at most) and thermodynamically accessible at room temperature, as experimentally confirmed by X-ray crystallography. However, II and IV are in general more stable relative to I in polar solvents (CHCl₃), presumably due to their higher dipole moments.

Our initial attempts to explore the potential of 2-6 as ligands for multinuclear transition-metal complexes prompted us to deprotonate the amidine moieties using "BuLi to generate bis(amidinates) for subsequent salt metathesis reactions (Scheme 2). We noted that THF solutions of 2 became substantially blue-emissive under exposure of UV light upon treatment with "BuLi due to the formation of [2Li₂]. The steady-state photoluminescence (PL) spectra of [2-5Li₂] confirm emission maxima between 421-441 nm and moderate Stokes shifts of 0.5-0.6 eV (Scheme 2, Table S11, and Figure S51-S56). The emission of the more conjugated bis-(amidinate) [6Li₂] is clearly red-shifted (λ_{max} = 485 nm). For a selected example (2^{2-}) the potential influence of the alkali metal cation on the emission was tested, and no significant effect observed. These results indicate that the bis(amidinate) moiety is the origin of the emission in THF solution, which is predominantly affected by the terminal aryl substituents.

In conclusion, five new N,N'-disubstituted ethylene-bridged bis(amidines) **2**–**6** with additional terminal N-donor sites were reported. As opposed to the sterically crowded bis(amidine) **1**,

The Journal of Organic Chemistry

Scheme 2. Deprotonation of 2-6 and Steady-State Emission Spectra of [2-6Li₂] and [2Na₂] in THF

2–6 exhibit unprecedented networks of weak to moderately strong inter- and intramolecular hydrogen bonds as demonstrated by IR spectroscopy and the XRD molecular structures of 3, 5, and 6. Careful examination of NMR-spectroscopic data revealed strong evidence for intramolecular hydrogen bonding being preserved in solution for 2–6, which was also confirmed by the calculated NH-¹H NMR shifts. Upon deprotonation with "BuLi or Na(NSiMe₃)₂, blue- and green-luminescent bis(amidinates) [2–6Li₂] and [2Na₂] were obtained. Present and future studies are concerned with the isolation of [2–6Li₂] and [2Na₂] as well as the exploration of the coordination behavior of 2–6 and their dianions toward late-transition-metal precursors in comparison with the large family of closely related 1,3,5-triazapentadienes/triazapentadienides to target novel photoluminescent clusters.

EXPERIMENTAL SECTION AND COMPUTATIONAL DETAILS

General Procedures. All synthetic procedures involving air- and moisture-sensitive compounds were carried out by using Schlenk techniques under an atmosphere of dry argon. Glassware was heatsealed with a heat gun under vacuum. Solvents: Prior to use, tetrahydrofuran (THF), diethyl ether, and toluene were freshly distilled from sodium/benzophenone. CH2Cl2 was distilled from CaH₂. Alternatively, the aforementioned solvents were purified using a PPT Solvent Purification System. For noninert manipulations, CH₂Cl₂, diethyl ether, and hexanes (mixture of isomers) were used as received without further purification. Deuterated solvents: CDCl₃ (Cambridge Isotope Laboratories, Inc., D, 99.8% + 0.03% v/v tetramethylsilane, TMS), C₆D₆ (Cambridge Isotope Laboratories, Inc., D, 99.5%), and THF-d₈ (Cambridge Isotope Laboratories, Inc., D, 99.5%) were used as received without further purification. Reactants: triethylamine (Alfa Aesar, 99%) was distilled from sodium before use; ethylenediamine (Alfa Aesar, >99%), pivaloyl chloride (Acros, 99%), PCl₅ (Alfa Aesar, 98%), mesitylamine (TCI, >99%), 4tert-butylaniline (Oakwood Chemicals, 98%), 2-aminopyridine (Alfa Aesar, 99%), 2-amino-6-methylpyridine (Alfa Aesar, 99%), 2-amino-4methylpyridine (Alfa Aesar, 98%), 2-amino-4,6-dimethylpyridine (Acros, 99%), 2-aminoquinoline (Ark Pharm, 98%), n-butyllithium (Acros, 1.6 M in hexanes), and NaN(SiMe₃)₂ (Alfa Aesar, 1.0 M in THF) were used as received without further purification. The synthesis of 1 was previously described. 10 Elemental analyses were performed by Atlantic Microlab, Inc. Melting points were determined with an SRS (Stanford Research Systems) Digi Melt instrument using open capillaries; values are uncorrected (the heating rate was 2 K/ min). NMR measurements were recorded on a Bruker DPX 300 and a Bruker Avance III 400 spectrometer at ambient probe temperatures unless otherwise noted. 13C{1H} NMR resonances were obtained with proton broadband decoupling and referenced to the solvent signals of CDCl₃ at 77.0 ppm, and C₆D₆ at 128.0 ppm (¹H NMR: 7.24 ppm (CHCl₃), 7.15 ppm (benzene), and 1.73 ppm (THF), respectively). ¹³C{¹H} NMR assignments are based on DEPT 135 and the following 2D experiments: COSY, NOESY, HSQC, and HMBC. Mass spectrometric analyses were performed on a VG70S double-focusing magnetic sector mass spectrometer (EI), on a Bruker Ultraflex II Tof instrument (MALDI), on a Waters Q-Tof API US quadrupole time-of-flight MS system (low resolution ESI), and on a Thermo Obitrap Velos Pro MS system (high resolution ESI). IR spectra were measured on a PerkinElmer Spectrum One FT-IR Spectrometer equipped with a Universal ATR Sampling Accessory. UV-vis spectra of solutions of 2-6, [2Li₂]-[6Li₂], and [2Na₂] in THF were measured with a Cary 60 spectrometer. Steady-state photoluminescence excitation and emission spectra of solutions of [2Li₂]-[6Li₂] and [2Na₂] in THF were recorded on a PTI Picomaster 1 fluorescence spectrometer system.

Synthesis of N,N'-1,2-Ethanediylbis(2,2-dimethylpropanamide), A. This compound was prepared in analogy to a literature procedure, with modifications:²⁶ Pivaloyl chloride (15.4 mL, 15.1 g, 125 mmol) was added dropwise via syringe to a solution of ethylenediamine (4.2 mL, 3.8 g, 63 mmol) and triethylamine (17.4 mL, 12.6 g, 125 mmol) in CH₂Cl₂ (100 mL) at 0 °C with stirring to form a colorless precipitate. The suspension was allowed to warm to room temperature for 10 min, heated to reflux for 8 h, and subsequently cooled to room temperature. The reaction mixture was washed with water (2 × 150 mL). The organic phase was separated and dried over anhydrous Na2SO4. Removal of the solvent by rotary evaporation yielded a colorless powder that was recrystallized from CH₂Cl₂ (80 mL) and dried by oil pump vacuum (20 h). Yield: 10.794 g (47.27 mmol, 76%). Mp: 116.5-118.0 °C. ¹H NMR (300.1 MHz, CDCl₃): δ 1.14 (s, 18 H, CH₃), 3.33–3.34 (m, 4 H, CH₂), 6.62 (broad s, 2 H, NH). ${}^{13}C\{{}^{1}H\}$ NMR (75.5 MHz, CDCl₃): δ 27.5 (CH₃), 38.5 (C, ^tBu), 40.4 (CH₂), 180.1 (C, C=O). IR (neat, cm⁻¹): 3295 (s, ν (N–H)), 3067 (w), 2970, 2955 (m, ν (C–H)), 2927, 2910, 2864 (w, ν (C-H)), 1631 (vs, ν (C=O)), 1542 (vs, δ (N-H)), 1478 (s), 1466 (m), 1443 (s), 1397 (m), 1362 (s), 1319 (m), 1297, 1243 (s), 1212 (vs), 1060, 1017 (w), 917 (m), 819, 788,

Synthesis of N,N'-1,2-Ethanediylbis(2,2-dimethylpropanimidoyl chloride), B. N,N'-1,2-Ethanediylbis(2,2-dimethylpropanamide) A (5.159 g, 22.59 mmol) and PCl₅ (9.465 g, 45.45 mmol) were dissolved in CH₂Cl₂ (60 mL) with stirring to give a pale yellow solution under evolution of HCl. After 3 d, a clear yellow solution had formed and all volatiles were removed in oil pump vacuum to leave a pale yellow green solid. Hexanes (60 mL) and then triethylamine (6.3 mL, 4.6 g, 45 mmol) were added. The resulting colorless suspension was stirred for 10 min and then filtered. The filter cake was washed with hexanes $(3 \times 10 \text{ mL})$. The volatiles of the filtrate were removed by oil pump vacuum to yield a pale yellow waxy oil. Yield: 5.148 g (19.41 mmol, 86%). ¹H NMR (300.1 MHz, CDCl₃): δ 1.19 (s, 18 H, CH₃), 3.67 (s, 4 H, CH₂). ^1H NMR (300.1 MHz, C₆D₆): δ 1.18 (s, 18 H, CH₃), 3.68 (s, 4 H, CH₂). 13 C{ 1 H} NMR (75.5 MHz, CDCl₃): δ 28.3 (CH₃), 43.5 (C, 1 Bu), 52.6 (CH₂), 153.4 (C, C=N). 13 C{ 1 H} NMR (75.5 MHz, C_6D_6): δ 28.4 (CH₃), 43.8 (C, ^tBu), 53.1 (CH₂), 152.9 (C, C=N). MS (CI in CH₄): m/z (relative intensity) 263 (1) $[M - H]^+$, 249 (1) $[M - CH_3]^+$, 229 (100) $[M - CI]^+$. HRMS (CI in CH₄): m/z calcd for C₁₂H₂₁N₂Cl₂ [M - H]⁺ 263.1082, found 263.1077. IR (neat, cm⁻¹): 2973 (m, ν (C–H)), 2933, 2912, 2872 (w,

 ν (C–H)), 1689 (s, ν (C=N)), 1606 (m), 1530 (w), 1478, 1459 (m), 1423, 1396 (w), 1365 (m), 1342 (w), 1276, 1246 (m), 1172 (w), 1100 (w), 1044 (m), 926 (vs), 872, 793 (s), 753 (w). Anal. Calcd for C₁₂H₂₂N₂Cl₂: C, 54.34; H, 8.36; N, 10.56. Found: C, 54.55; H, 8.60; N, 10.47.

General Procedure for the Preparation of 2-6. A solution of arylamine (19.42 mmol) in toluene (10-30 mL, a) was added dropwise to a solution of N_1N' -1,2-ethanediylbis(2,2-dimethylpropanimidoyl chloride) B (9.80 mmol) in toluene (40 mL, b) with stirring (5) or b was added dropwise to a (2-4, 6). The reaction mixture was heated at 80 °C for 72 h (2-4) or to reflux for 24 h (5-6), cooled to room temperature, and filtered. The filter cake was washed with cold (0 °C) toluene (3–5 × 10 mL), then with diethyl ether (3 × 5 mL) and finally suspended in a mixture of diethyl ether (4: 300 mL; 2: 150 mL; 3, 5, 6: 100 mL) and a saturated aqueous Na₂CO₃ solution (100 mL), which was stirred for 30 min. The organic phase was separated, washed with water $(3-5 \times 100 \text{ mL})$, and dried over anhydrous Na₂SO₄ (2-5). Subsequent filtration and removal of all volatiles from the filtrate by rotary evaporation resulted in a colorless solid that was recrystallized from a mixture of hexanes and diethyl ether (5) and dried in oil pump vacuum for 24 h (5). Alternatively, the filtrate was concentrated to approximately 20 mL by rotary evaporation and then layered with hexanes (40 mL) 2-4, which caused the formation of colorless crystals (-5 °C, 24 h) that were isolated by filtration, washed with cold (0 °C) hexanes (3 \times 5 mL), and dried in oil pump vacuum for 48 h (2-4). For 6, the reduction of diethyl ether by 20mL caused a precipitate to form which was isolated by filtration and dried in oil pump vacuum for 24 h.

2. This bis(amidine) was obtained by slow crystallization from diethyl ether/hexanes (-5 °C, 24 h). Yield: 54%. Mp: 150.8-151.0 °C. ¹H NMR (400.1 MHz, CDCl₃): δ 1.20 (s, 18 H, CH₃, ^tBu), 3.06 (s, 4 H, CH₂), 5.68 (broad s, 2 H, NH), 6.69 (d, ${}^{3}J_{H,H}$ = 8.1 Hz, 2 H; py H³), 6.73 (t, ${}^{3}J_{H,H}$ = 6.0 Hz, 2 H; py H⁵), 7.44 (t, ${}^{3}J_{H,H}$ = 6.9 Hz, 2 H; py H⁴), 8.21 (d, ${}^{3}J_{H,H}$ = 3.8 Hz, 2 H; py H⁶). ${}^{1}H$ NMR (400.1 MHz, C₆D₆): δ 1.25 (s, 18 H, CH₃, ^tBu), 3.05 (s, 4 H, CH₂), 6.44 (t, ³J_{H.H} = 5.9 Hz, 2 H; py H⁵), 6.58 (broad s, 2 H, NH), 6.80 (d, ³J_{H.H} = 7.6 Hz, 2 H; py H³), 7.10 (t, ${}^{3}J_{H,H}$ = 7.0 Hz, 2 H; py H⁴), 8.23 (d, $J_{H,H}$ = 2.4 Hz, 2 H; py H⁶). ${}^{13}C\{{}^{1}H\}$ NMR (100.6 MHz, CDCl₃): δ 29.2 (CH₃), 39.1 (C, ^tBu), 43.5 (CH₂), 116.1 (CH, py C⁵), 116.9 (CH, py C³), 136.8 (CH, py C⁴), 147.9 (CH, py C⁶), 162.9 (C, CN₂), 163.3 (C, py C²). ${}^{13}C{}^{1}H}$ NMR (100.6 MHz, C₆D₆): δ 29.4 (CH₃), 39.2 (C, ^tBu), 43.5 (CH₂), 115.9 (CH, py C⁵), 117.8 (CH, py C³), 136.6 (CH, py C⁴), 147.7 (CH, py C⁶), 163.4 (C, CN₂), 164.1 (C, py C²). MS (ESI(+)): m/z (relative intensity): 381 (62) [M + H]⁺, 191 (100) $[M + 2 H]^{2+}$. HRMS (ESI(+)): m/z calcd for $C_{22}H_{33}N_6$ [M +H]⁺ 381.2767, found 381.2765. IR (neat, cm⁻¹): 3266 (w, ν (N–H)), 3044 (w), 2955 (m), 2918, 2906, 2871 (w, (ν-C-H)), 1624 (vs), 1583, 1544, 1527, 1464, 1421 (vs), 1398 (m), 1365, 1356, 1334, 1303 (m), 1285, 1269 (s), 1225, 1203, 1191, 1146 (m), 1108, 1097, 1074, 1055, 1044, 1018 (w), 991, 907 (m), 868 (w), 827 (m), 788 (w), 766 (m), 740 (vs), 630, 614 (m). UV-vis (THF): λ [nm] (ε [L·mol⁻¹· cm⁻¹]) 237, 1.80 × 10^4 ; \approx 297, 9.56 × 10^3 (br shoulder). Anal. Calcd for C22H32N6: C, 69.44; H, 8.48; N, 22.09. Found: C, 69.40; H, 8.58; N, 21.88.

3. This bis(amidine) was obtained by slow crystallization from diethyl ether/hexanes (-5 °C, 24 h). Yield: 61%. Mp: 165.2–167.6 °C. 1 H NMR (400.1 MHz, CDCl₃): δ 1.18 (s, 18 H, CH₃, 1 Bu), 2.40 (s, 6 H, CH₃, 6-py), 3.09 (s, 4 H, CH₂), 5.57 (broad s, 2 H, NH), 6.44 (d, $^3J_{\rm HH}$ = 7.3 Hz, 2 H, CH, py H³), 6.60 (d, $^3J_{\rm HH}$ = 7.3 Hz, 2 H, CH, py H⁵), 7.33 (t, $^3J_{\rm HH}$ = 7.7 Hz, 2 H, CH, py H⁴). 1 H NMR (400.1 MHz, C₆D₆): δ 1.25 (s, 18 H, CH₃, 1 Bu), 2.36 (s, 6 H, CH₃, 6-py), 3.07–3.10 (m, 4 H, CH₂), 6.39 (d, $^3J_{\rm HH}$ = 7.3 Hz, 2 H, CH, py H⁵), ≈ 6.60 (broad s, 2 H, NH), 6.69 (d, $^3J_{\rm HH}$ = 8.0 Hz, 2 H, CH, py H³), 7.10 (t, $^3J_{\rm HH}$ = 7.7 Hz, 2 H, CH, py H⁴). 13 C{ 1 H} NMR (100.6 MHz, CDCl₃): δ 24.4 (CH₃, 6-py), 29.3 (CH₃, 1 Bu), 39.1 (C, 1 Bu), 43.5 (CH₂), 113.4 (CH, py C³), 115.3 (CH, py C⁵), 136.9 (CH, py C⁴), 156.5 (C, py C⁶), 162.7 (2 × C, py C², CN₂). 13 C{ 1 H} NMR (100.6 MHz, C₆D₆): δ 24.4 (CH₃, 6-py), 29.5 (CH₃, 1 Bu), 39.2 (C, 1 Bu), 43.5 (CH₂), 114.7 (broad, CH, py C³), 115.0 (CH, py C⁵), 137.0 (CH, py C⁴), 156.1 (C, py C⁶), 163.2 (C, CN₂), 163.5 (C, py C²).

MS (ESI(+)): m/z (relative intensity): 409 (69) [M + H]⁺, 205 (100) [M + 2 H]²⁺. HRMS (ESI(+)): m/z calcd for $C_{24}H_{37}N_6$ [M + H]⁺ 409.3080, found 409.3074. IR (neat, cm⁻¹): 3308 (m, ν (N-H)), 3058, 3042, 2966 (w, $(\nu$ -C-H)), 2955 (m, $(\nu$ -C-H)), 2922, 2904, 2870 (w, $(\nu$ -C-H)), 1617 (vs), 1584 (s), 1556, 1522, 1437 (vs), 1397, 1368 (m), 1327 (s), 1305, 1277 (m), 1224, 1154 (s), 1111 (w), 1090 (m), 1070, 1048, 1033, 988, 940 (w), 878 (s), 860, 822 (m), 777 (s), 752 (m), 738 (s), 718, 627 (m). UV-vis (THF): λ [nm] (ε [L·mol⁻¹·cm⁻¹]) 239, 1.69 × 10⁴; 293, 1.26 × 10⁴. Anal. Calcd for $C_{24}H_{36}N_6$: C, 70.55; H, 8.88; N, 20.57. Found: C, 70.27; H, 9.08; N, 20.45.

4. This bis(amidine) was obtained by slow crystallization from diethyl ether/hexanes (-5 °C, 24 h). Yield: 56%. Mp: 184.6-185.9 °C. ¹H NMR (400 MHz, CDCl₃): δ 1.20 (s, 18 H, CH₃, ^tBu), 2.21 (s, 6 H, CH₃, 6-py), 3.01 (s, 4 H, CH₂), 5.69 (broad s, 2H, NH), 6.51 (s, 2 H, CH, py H³), 6.56 (d, ${}^{3}J_{HH}$ = 4.6 Hz, 2 H, CH, py H⁵), 8.06 (d, $^{3}J_{HH} = 4.7 \text{ Hz}, 2 \text{ H, CH, py H}^{6}$. $^{1}\text{H NMR} (400.1 \text{ MHz}, \text{C}_{6}\text{D}_{6}): \delta 1.31$ (s, 18 H, CH₃, ^tBu), 1.89 (s, 6 H, CH₃, 6-py), 3.07 (s, 4 H, CH₂), 6.34 (d, ${}^{3}J_{HH}$ = 5.0 Hz, 2 H, CH, py H⁵), 6.71 (s, 2 H, CH, py H³), \approx 6.71 (broad s, overlaid by py H³ signal, 2H, NH), 8.17 (d, ${}^{3}J_{HH}$ = 5.1 Hz, 2 H, CH, py H⁶). ${}^{13}C\{{}^{1}H\}$ NMR (100.6 MHz MHz, CDCl₃): δ 20.9 (CH₃, 4-py), 29.2 (CH₃, ^tBu), 39.0 (C, ^tBu), 43.5 (CH₂), 117.2 (CH, py $C^{\overline{3}}$), 117.5 (CH, py C^{5}), 147.4 (CH, py C^{6}), 147.7 (C, py C⁴), 162.7, 163.3 (C, CN₂, py C²). ¹³C{¹H} NMR (100.6 MHz MHz, C_6D_6): δ 20.7 (CH₃, 4-py), 29.5 (CH₃, ^tBu), 39.2 (C, ^tBu), 43.5 (CH₂), 117.3 (CH, py C^5), 118.3 (CH, py C^3), 147.4 (C, CH, py $C^{4,6}$), 163.3 (C, CN_2), 164.2 (C, py C^2). MS (ESI(+)): m/z(relative intensity): 409 (79) $[M + H]^+$, 205 (100) $[M + 2 H]^{2+}$. HRMS (ESI(+)): m/z calcd for $C_{24}H_{37}N_6$ [M + H]⁺ 409.3080, found 409.3074. IR (neat, cm $^{-1}$): 3283, 3267, 3252 (w, ν (N–H)), 3046, 2961(m, $(\nu$ -C-H)), 2924, 2867 (w, $(\nu$ -C-H)), 1624 (vs), 1596, 1534 (vs), 1475, 1463, 1395 (s), 1363, 1330, 1303, 1226, 1210, 1159 (m), 1113, 1071, 1049, 1035, 1012, 990, 943 (w), 889, 866, 816 (m), 801 (s), 768, 736, 659 (w), 634 (m). UV-vis (THF): λ [nm] (ε [L· $\text{mol}^{-1}\cdot\text{cm}^{-1}$) 242, 2.44 × 10⁴; \approx 276, 2.15 × 10⁴ (br shoulder). Anal. Calcd for C₂₄H₃₆N₆: C, 70.55; H, 8.88; N, 20.57. Found: C, 70.65; H,

5. This bis(amidine) was obtained by recrystallization from a mixture of hexanes and diethyl ether (40 mL, 1:3 v/v) at -37 °C within 3 days as a colorless crystalline solid. Yield: 63%. Mp: 148.2-151.9 °C. ¹H NMR (400.1 MHz, CDCl₃): δ 1.17 (s, 18 H, CH₃, ^tBu), 2.17 (s, 6 H, CH₃, 4-py), 2.35 (s, 6 H, CH₃, 6-py), 3.05 (s, 4 H, CH₂), 5.58 (broad s, 2 H, NH), 6.29 (s, 2 H, CH, py H³), 6.45 (s, 2 H, CH, py H⁵). ¹H NMR (400.1 MHz, C_6D_6): δ 1.32 (s, 18 H, CH_3 , ^tBu), 1.92 (s, 6 H, CH₃, 4-py), 2.37 (s, 6 H, CH₃, 6-py), 3.09 (s, 4 H, CH₂), 6.25 (s, 2 H, CH, py H⁵), 6.60 (s, 2 H, CH, py H³), \approx 6.90 (broad s, 2 H, NH). ${}^{13}\text{C}\{{}^{1}\text{H}\}$ NMR (100.6 MHz, CDCl₃): δ 20.8 (CH₃, 4-py), 24.2 (CH₃, 6-py), 29.3 (CH₃, ^tBu), 39.0 (C, ^tBu), 43.5 (CH₂), 113.9 (CH, py C³), 116.7 (CH, py C⁵), 147.8 (C, py C⁴), 156.1 (C, py C⁶), 162.5, 162.8 (C, CN₂, py C²). 13 C{ 14 H} NMR (100.6 MHz, C₆D₆): δ 20.7 (CH₃, 4-py), 24.2 (CH₃, 6-py), 29.5 (CH₃, ^tBu), 39.2 (C, ^tBu), 43.4 (CH₂), 115.3 (CH, py C³), 116.5 (CH, py C⁵), 147.6 (C, py C⁴), 155.7 (C, py C⁶), 163.0 (C, CN₂), 163.7 (C, py C²). MS (ESI(+)): m/z (relative intensity): 437 (22) [M + H]⁺, 219 (100) [M + 2 H]²⁺. HRMS (ESI(+)): m/z calcd for $C_{26}H_{41}N_6$ [M + H]⁺ 437.3393, found 437.3386. IR (neat, cm⁻¹): 3309 (w, ν (N–H)), 3039 (w), 2960 (m, (ν -C–H)), 2924, 2870 (w, (ν -C–H)), 1627 (vs), 1599, 1543, 1525 (vs), 1488, 1456 (m), 1399, 1344 (s), 1301 (w), 1222 (s), 1194 (m), 1154 (w), 1112, 1032, 989, 962, 942 (w), 878 (s), 855, 831, 808, 733, 657, 608 (m). UV–vis (THF): λ [nm] (ε [L·mol⁻¹·cm⁻¹]) 240, 2.06 $\times 10^4$; ≈ 292 , 1.58 $\times 10^4$ (br shoulder). Anal. Calcd for $C_{26}H_{40}N_6$: C, 71.52; H, 9.23; N, 19.25. Found: C, 71.79; H, 9.31; N, 18.95.

6. This bis(amidine) was obtained by precipitation from diethyl ether (80 mL) as a colorless powder. Yield: 58%. Mp: 222.1–222.4 °C. ¹H NMR (400.1 MHz, CDCl₃): δ 1.21 (s, 18 H, CH₃, ¹Bu), 3.20 (s, 4 H, CH₂), 5.99 (broad s, 2 H, NH), 6.87 (d, ${}^{3}J_{\text{HH}}$ = 8.4 Hz, 2 H, CH, quin H³), 7.30 (t, ${}^{3}J_{\text{HH}}$ = 7.4 Hz, 2 H, CH, quin H⁶), 7.55 (t, ${}^{3}J_{\text{HH}}$ = 7.5 Hz, 2 H, CH, quin H⁷), 7.64 (d, ${}^{3}J_{\text{HH}}$ = 7.8 Hz, 2 H, CH, quin H⁵), 7.80 (d, ${}^{3}J_{\text{HH}}$ = 8.3 Hz, 2 H, CH, quin H⁸), 7.87 (d, ${}^{3}J_{\text{HH}}$ = 8.6 Hz, 2 H, CH, quin H⁴). ¹H NMR (400.1 MHz, C_6D_6): δ 1.27 (s, 18

H, CH₃, ${}^{t}Bu$), 3.07 (s, 4 H, CH₂), 7.03 (d, ${}^{3}J_{HH}$ = 8.6 Hz, 2 H, CH, quin H³), 7.10 (t, ${}^{3}J_{HH}$ = 7.4 Hz, 2 H, CH, quin H⁶), 7.37–7.41 (m, 4 H, CH, quin H^{5,7}), 7.50 (d, ${}^{3}J_{HH}$ = 8.7 Hz, 2 H, CH, quin H⁴), 8.02 (d, ${}^{3}J_{HH}$ = 8.5 Hz, 2 H, CH, quin H⁸). ${}^{13}C\{{}^{1}H\}$ NMR (100.6 MHz, CDCl₃): δ 29.2 (CH₃, ^tBu), 39.2 (C, ^tBu), 43.4 (CH₂), 118.8 (CH₃) quin C³), 123.6 (CH, quin C⁶), 124.6 (C, quin C^{4a}), 127.2 (CH, quin C^{5}), 127.4 (CH, quin C^{8}), 129.1 (CH, quin C^{7}), 136.5 (CH, quin C^{4}), 147.4 (C, quin C^{8a}), 162.4 (C, quin C^{2}), 163.5 (C, C^{8a}). $C^{13}C^{14}$ NMR (100.6 MHz, $C^{6}D_{6}$): C^{6} 29.4 (CH₃, C^{6} Bu), 39.2 (C, C^{6} Bu), 43.4 (CH₂), 120.2 (CH, quin C³), 123.7 (CH, quin C⁶), 125.1 (C, quin C^{4a}), 127.6–129.4 (CH, overlaid by C_6D_6/C_6H_6 signal, quin $C^{5,7,8}$), 136.5 (CH, quin C^4), 148.1 (C, quin C^{8a}), 162.9 (C, quin C^2), 164.6 (C, CN_2). MS (ESI(+) in MeOH): m/z (relative intensity): 481 (24) $[M + H]^+$, 241 (100) $[M + 2 H]^{2+}$. HRMS (ESI(+)): m/zcalcd for $C_{30}H_{37}N_6$ [M + H]⁺ 481.3080, found 481.3072. IR (neat, cm⁻¹): 3275 (w, ν (N-H)), 3040 (w), 2960 (m, (ν -C-H)), 2925, 2903, 2868 (w, $(\nu$ -C-H)), 1629 (m), 1596 (vs), 1551 (s), 1530 (vs), 1498 (m), 1464, 1417 (s), 1396 (w), 1377 (s), 1349 (m), 1302 (s), 1262 (m), 1246 (w), 1223, 1188 (m), 1143, 1120 (w), 1103, 1068, 1048, 1022, 962, 928, (w), 863, 831, 803, 782, 713 (m), 684 (w), 618 (s). UV-vis (THF): λ [nm] (ε [L·mol⁻¹·cm⁻¹]) 249, 4.49 × 10⁴; 342, 1.37×10^4 . Anal. Calcd for $C_{30}H_{36}N_6$: C, 74.97; H, 7.55; N, 17.48. Found: C, 74.69; H, 7.36; N, 17.71.

Deprotonation Studies of 2–6. A 1.6 M solution of *n*-butyllithium in hexanes (0.03 mL, 0.05 mmol) or a 1.0 M solution of NaN(SiMe₃)₂ in THF (0.05 mL, 0.05 mmol) was added dropwise to a solution of **2–6** (0.024 mmol) in THF (12 mL) at -78 °C with stirring. After 15 min, the reaction mixture was allowed to warm to room temperature for 2 h and then diluted if required (UV–vis: 1.0–2.6 × 10⁻⁵ M, excitation and emission spectra: 5.2 × 10⁻⁵–1.8 × 10⁻⁴ M; see Table S11). UV–vis (THF): λ [nm] (ε [L·mol⁻¹·cm⁻¹]) [2Li₂]: 257, 2.70 × 10⁴; ≈295, 2.21 × 10⁴ (br shoulder); [2Na₂]: 258, 2.98 × 10⁴; ≈295, 2.48 × 10⁴ (br shoulder); [3Li₂]: 253, 2.82 × 10⁴; 296, 2.79 × 10⁴; [4Li₂]: 249, 2.92 × 10⁴; ≈274, 2.82 × 10⁴ (br shoulder); [5Li₂]: UV–vis (THF): 253, 2.73 × 10⁴; 280, 2.59 × 10⁴; [6Li₂]: 250, 9.48 × 10⁴; 342, 3.04 × 10⁴.

X-ray Crystallography. Single crystals of 3 were grown as colorless blocks from a THF solution that was layered with hexanes and stored at −35 °C. Colorless blocks of 5·C₆D₆ were obtained from slowly concentrating C₆D₆/hexanes solutions at room temperature. Colorless needles of 6 were obtained by allowing diethyl ether vapor to slowly diffuse into a CH₂Cl₂ solution at room temperature. X-ray data for 3 were collected on a Bruker APEX diffractometer and for 5. C₆D₆ and 6 on a Bruker Venture X-ray diffractometer (graphitemonochromated Cu K α radiation, $\lambda = 1.54178$ Å or graphitemonochromated Mo K α radiation, $\lambda = 0.71073$ Å) by using ω and φ scans at 110 K (3) or 100 K (5 \cdot C₆D₆ and 6, Table S1). The integrated intensities for each reflection were obtained by reduction of the data frames with the program APEX2 (3) or APEX3 (5·C₆D₆, and 6). Cell parameters were obtained and refined with 13527 (5195 unique, 3), 19670 (3840 unique, $5 \cdot C_6 D_6$), and 5131 (2686 unique, 6) reflections, respectively. The integrated intensity information for each reflection was obtained by reduction of the data frames by using APEX2 (3) or APEX3 (5· C_6D_6 , and 6). The integrated data for 3 and 5·C₆D₆ were corrected for absorption by using SADABS.²⁸ For 6, TWINABS²⁹ was used for integrated data correction as well as to generate TWIN4.hkl, reflections from the major twin component. This data was used for structure solution as well as for final leastsquares refinement. The structures were solved by direct methods and refined (weighted least-squares refinement on F2) by using SHELXL-97.30 The hydrogen atoms were placed in idealized positions and refined by using a riding model. Non-hydrogen atoms were refined with anisotropic thermal parameters. For 5·C₆D₆, elongated thermal ellipsoids on atoms C20 through C26, N6, C 1s through C6s indicated disorder, which were modeled successfully between two positions each with an occupancy ratio of 0.51:0.49. Appropriate restraints and constraints were added to keep the bond distances, angles, and thermal ellipsoids meaningful. For 6, extremely elongated thermal ellipsoids on atoms C27, C28, and C29 indicated disorder and were modeled successfully between two positions each with an

occupancy ratio of 0.70:0.30. Appropriate restraints and/or constraints were added to keep the bond distances, angles, and thermal ellipsoids meaningful. For all structures, the absence of additional symmetry and void was confirmed using PLATON (ADDSYM).³¹

Computational Details. All structures (1-6) were fully geometry-optimized using the Gaussian 09 software package (G09) and employing an ultrafine grid (99590) for enhanced accuracy. Density functional theory was used with the B3LYP functional³³ and a triple- ζ quality basis set (6-311G(d)), including extra polarization functions.³⁴ No symmetry constraints were imposed on any structures during optimization. Frequency calculations were performed on the B3LYP/6-311G(d)-optimized geometries for all species to establish the nature of each structure. All isomers were local minima by inspecting the number of imaginary frequencies ($I_{\rm m}$ = 0). However, a few species presented a very small imaginary mode(s) (<1-20 cm⁻¹) which was caused by the rotation of the tert-butyl group(s). These small frequencies did not significantly impact the relative stability. For NMR computations, the gauge-independent atomic orbital (GIAO) method was used as implemented in the G09 suite³² or in Turbomole v7.2.³⁵ For Gaussian the CAM-B3LYP functional³⁶ was used together with a basis set incorporating more diffuse functions (6-311+ +G(d)),³⁴ whereas for Turbomole the B-P86^{33a,37} and B3LYP³³ functionals were used together with the RIDFT module³⁸ and the basis sets def-SV(P)³⁹ and def2-TZVP.⁴⁰ See Tables S7–S9 for selected computed ¹H NMR chemical shifts referenced to TMS.

ASSOCIATED CONTENT

S Supporting Information

The Supporting Information is available free of charge on the ACS Publications website at DOI: 10.1021/acs.joc.9b01908.

Crystallographic data, computational details, ¹H and ¹³C{¹H} NMR spectra of B, and 2–6, UV–vis spectra of 2–6, [2–6Li₂], and [2Na₂], steady-state photoluminescence excitation and emission spectra of [2–6Li₂], and [2Na₂] (PDF)

X-ray data for compound 3 (CIF)

X-ray data for compound $5 \cdot C_6 D_6$ (CIF)

X-ray data for compound 6 (CIF)

Computed structure coordinates (XYZ)

AUTHOR INFORMATION

Corresponding Author

* E-mail: michael.stollenz@kennesaw.edu.

ORCID 6

Andreas Ehnbom: 0000-0002-7044-1712 Michael Stollenz: 0000-0002-8635-164X

Notes

The authors declare no competing financial interest. CCDC 1920484 (3), 1920485 (5·C₆D₆), and 1920483 (6) contain the supplementary crystallographic data for this paper. These data can be obtained free of charge via www.ccdc.cam. ac.uk/data_request/cif, or by emailing data_request@ccdc.cam.ac.uk, or by contacting The Cambridge Crystallographic Data Centre, 12 Union Road, Cambridge CB2 1EZ, UK; fax: + 44 1223 336033.

ACKNOWLEDGMENTS

We thank Alvaro Calderón Díaz, Nimia Zoé Maya, Ofumere Omokhodion, Nattasith Siwabut, and Allan Nguyen for experimental assistance. Dr. Michael D. Walla and Dr. William E. Cotham (Mass Spectrometry Center at the University of South Carolina) are acknowledged for recording mass spectra. We are grateful to Dr. Michael B. Hall, Dr. Lisa M. Pérez, the

Laboratory for Molecular Simulations, and the Texas A&M Supercomputing Facility for providing computing resources. A.E. acknowledges financial support by NSF Grant Nos. CHE-1566601 and CHE-1664866. The Department of Chemistry and Biochemistry and the College of Sciences and Mathematics (CSM) at Kennesaw State University are acknowledged for financial support (New Faculty Startup Fund (No. 08020) and the CSM Research Stimulus Program). Aditya Birla Carbon is acknowledged for a Birla Carbon Scholarship (O.U.T.). This material is based upon work supported by the National Science Foundation under Grant No. CHE-1800332.

REFERENCES

(1) Häfelinger, G.; Kuske, F. K. H. In The Chemistry of Amidines and Imidates; Patai, S., Rappoport, Z., Eds.; John Wiley & Sons, Ltd.: Chichester, UK, 1991; pp 1-100.

(2) (a) Lindauer, D.; Beckert, R.; Döring, M.; Fehling, P.; Görls, H. On the Aminolysis of Bis-Imidoylchlorides of Oxalic Acid. Part I. Reaction with Aromatic and Aliphatic Amines. J. Prakt. Chem. 1995, 337, 143-152. (b) Lindauer, D.; Beckert, R.; Billert, T.; Döring, M.; Görls, H. On the Aminolysis of Bis-Imidoylchlorides of Oxalic Acid. 11. Reaction with Aliphatic Diamines and Aminoalcohols. J. Prakt. Chem. 1995, 337, 508-515. (c) Atzrodt, J.; Brandenburg, J.; Käpplinger, C.; Beckert, R.; Günther, W.; Görls, H.; Fabian, J. 5-Ring-Cycloamidines - Deeply Coloured Heterocycles with Unusual Properties. I. Synthesis and Spectral Features. J. Prakt. Chem. 1997, 339, 729-734. (d) Müller, D.; Beckert, R.; Görls, H. Bis-Amidines as Useful Building Blocks for Heterofulvenes and - Fulvalenes. Synthesis 2001, 4, 601-606. (e) Matschke, M.; Beckert, R.; Kubicova, L.; Biskup, C. The Introduction of OH and COOH Groups into 4H-Imidazoles: Water-Soluble Functional Dyes and Quinomethides. Synthesis 2008, 2957-2962. (f) Strathausen, R.; Beckert, R.; Fleischhauer, J.; Müller, D.; Görls, H. Novel Dihydropyrazines and their Double ortho-Annulation to Hexaazapentacenes. Z. Naturforsch., B: J. Chem. Sci. 2014, 69b, 641-649.

(3) (a) Barker, J.; Kilner, M. The coordination chemistry of the amidine ligand. Coord. Chem. Rev. 1994, 133, 219-300. (b) Edelmann, F. T. N-silylated benzamidines: versatile building blocks in main group and coordination chemistry. Coord. Chem. Rev. 1994, 137, 403-481. (c) Coles, M. P. Application of neutral amidines and guanidines in coordination chemistry. Dalton Trans. 2006, 985-1001. (d) Edelmann, F. T. In Adv. Organometallic Chemistry; Hill, A. F., Fink, M. J., Eds.; Elsevier: Amsterdam, 2008; Vol 57, pp 183-352. (4) Hill, A. J.; Johnston, J. V. Amidines Derived from Ethylenedi-

amine. I. Diamidines. J. Am. Chem. Soc. 1954, 76, 920-922.

(5) (a) Wild, F. R. W. P.; Zsolnai, L.; Huttner, G.; Brintzinger, H. H. ansa-Metallocene derivatives IV. Synthesis and molecular structures of chiral ansa-titanocene derivatives with bridged tetrahydroindenyl ligands. J. Organomet. Chem. 1982, 232, 233-247. (b) Wild, F. R. W. P.; Wasiucionek, M.; Huttner, G.; Brintzinger, H. H. ansa-Metallocene derivatives: VII. Synthesis and crystal structure of a chiral ansazirconocene derivative with ethylene-bridged tetrahydroindenyl ligands. J. Organomet. Chem. 1985, 288, 63-67. (c) Collins, S.; Kuntz, B. A.; Taylor, N. J.; Ward, D. G. X-Ray structures of ethylenebis(tetrahydroindenyl)-titanium and -zirconium dichlorides: a revision. J. Organomet. Chem. 1988, 342, 21-29. (d) Brintzinger, H. H.; Fischer, D.; Mülhaupt, R.; Rieger, B.; Waymouth, R. M. Stereospecific Olefin Polymerization with Chiral Metallocene Catalysts. Angew. Chem., Int. Ed. Engl. 1995, 34, 1143-1170. (e) Halterman, R. L. Synthesis and applications of chiral cyclopentadienylmetal complexes. Chem. Rev. 1992, 92, 965-994. (f) Shapiro, P. J. The evolution of the ansa-bridge and its effect on the scope of metallocene chemistry. Coord. Chem. Rev. 2002, 231, 67-81. (g) Hoveyda, A. H.; Morken, J. P. Enantioselective C-C and C-H Bond Formation Mediated or Catalyzed by Chiral ebthi Complexes of Titanium and Zirconium. Angew. Chem., Int. Ed. Engl. 1996, 35, 1262-1284. (h) Qian, Y.; Huang, J.; Bala, M. D.; Lian, B.;

Zhang, H.; Zhang, H. Synthesis, Structures, and Catalytic Reactions of Ring-Substituted Titanium(IV) Complexes. Chem. Rev. 2003, 103, 2633-2690. (i) Prashar, S.; Antiñolo, A.; Otero, A. Insights into group 4 and 5 ansa-bis(cyclopentadienyl) complexes with a singleatom bridge. Coord. Chem. Rev. 2006, 250, 133-154. (j) Cobzaru, C.; Hild, S.; Boger, A.; Troll, C.; Rieger, B. "Dual-side" catalysts for high and ultrahigh molecular weight homopolypropylene elastomers and plastomers. Coord. Chem. Rev. 2006, 250, 189-211. (k) Wang, B. Ansa-metallocene polymerization catalysts: Effects of the bridges on the catalytic activities. Coord. Chem. Rev. 2006, 250, 242-258. (1) Erker, G. Syntheses and reactions of fulvene-derived substituted aminoalkyl-Cp and phosphinoalkyl-Cp-Group 4 metal complexes. Coord. Chem. Rev. 2006, 250, 1056-1070.

(6) (a) Whitener, G. D.; Hagadorn, J. R.; Arnold, J. Synthesis and characterization of a new class of chelating bis(amidinate) ligands. J. Chem. Soc., Dalton Trans. 1999, 1249-1255. (b) Hill, M. S.; Hitchcock, P. B.; Mansell, S. M. Racemic N-aryl bis(amidines) and bis(amidinates): on the trail of enantioselective organolanthanide catalysts. Dalton Trans. 2006, 1544-1553. (c) Ohashi, M.; Yagyu, A.; Yamagata, T.; Mashima, K. Tetraplatinum precursors for supramolecular assemblies: syntheses, crystal structures, and stereoselective self-assemblies of $[Pt_4(\mu\text{-OCOCH}_3)_6(\kappa^4\text{-}N_4\text{-DArBp})]$ (DArBp = 1,3bis(arylbenzamidinate)propane). Chem. Commun. 2007, 3103-3105. (7) (a) Hagadorn, J. R.; Arnold, J. Tethered Bis-Amidinates as Supporting Ligands: A Concerted Elimination/ σ - π Rearrangement Reaction Forming an Unusual Titanium Arene Complex. Angew. Chem., Int. Ed. 1998, 37, 1729-1731. (b) Babcock, J. R.; Incarvito, C.; Rheingold, A. L.; Fettinger, J. C.; Sita, L. R. Double Heterocumulene Metathesis of Cyclic Bis(trimethylsilylamido)stannylenes and Tethered Bimetallic Bisamidinates from the Resulting α , ω -Biscarbodiimides. Organometallics 1999, 18, 5729-5732. (c) Bambirra, S.; Meetsma, A.; Hessen, B.; Teuben, J. H. Yttrium Alkyl Complex with a Linked Bis(amidinate) Ancillary Ligand. Organometallics 2001, 20, 782-785. (d) Li, J.-F.; Huang, S.-P.; Weng, L.-H.; Liu, D.-S. Synthesis and structural studies of some titanium and zirconium complexes with chiral bis(amide), amidinate or bis(amidinate) ligands. J. Organomet. Chem. 2006, 691, 3003-3010. (e) Wang, J.; Cai, T.; Yao, Y.; Zhang, Y.; Shen, Q. Ytterbium amides of linked bis(amidinate): synthesis, molecular structures, and reactivity for the polymerization of Llactide. Dalton Trans. 2007, 5275-5281. (f) Yan, L.; Liu, H.; Wang, J.; Zhang, Y.; Shen, Q. Divalent Lanthanide Complexes Supported by the Bridged Bis(amidinates) L [L = $Me_3SiN(Ph)CN(CH_2)_3NC(Ph)$ -NSiMe₃]: Synthesis, Molecular Structures and One-Electron-Transfer Reactions. Inorg. Chem. 2012, 51, 4151-4160. (g) Tolpygin, A. O.; Shavyrin, A. S.; Cherkasov, A. V.; Fukin, G. K.; Trifonov, A. A. Chloro and Alkyl Rare-Earth Complexes Supported by ansa-Bis(amidinate) Ligands with a Rigid o-Phenylene Linker. Ligand Steric Bulk: A Means of Stabilization or Destabilization? Organometallics 2012, 31, 5405-5413. (h) Tolpygin, A. O.; Skvortsov, G. G.; Cherkasov, A. V.; Fukin, G. K.; Glukhova, T. A.; Trifonov, A. A. Lanthanide Borohydrido Complexes Supported by ansa-Bis(amidinato) Ligands with a Rigid o-Phenylene Linker: Effect of Ligand Tailoring on Catalytic Lactide Polymerization. Eur. J. Inorg. Chem. 2013, 6009-6018. (i) Tolpygin, A. O.; Cherkasov, A. V.; Fukin, G. K.; Trifonov, A. A. Reversible Switching of Coordination Mode of ansa bis-(Amidinate) Ligand in Ytterbium Complexes Driven by Oxidation State of the Metal Atom. Inorg. Chem. 2014, 53, 1537-1543. (j) Skvortsov, G. G.; Tolpygin, A. O.; Fukin, G. K.; Long, J.; Larionova, J.; Cherkasov, A. V.; Trifonov, A. A. Rare-Earth Complexes Coordinated by ansa-Bis(amidinate) Ligands with m-Phenylene, 2,6-Pyridinediyl, and SiMe2 Linkers. Eur. J. Inorg. Chem. 2017, 4275-4284.

- (8) Kawaguchi, H.; Matsuo, T. Binuclear iron(II) complex from a linked-bis(amidinate) ligand: synthesis and its reaction with carbon monoxide. Chem. Commun. 2002, 958-959.
- (9) Stollenz, M. Linear Copper Complex Arrays as Versatile Molecular Strings: Syntheses, Structures, Luminescence, and Magnetism. Chem. - Eur. J. 2019, 25, 4274-4298.

(10) Stollenz, M.; Raymond, J. E.; Pérez, L. M.; Wiederkehr, J.; Bhuvanesh, N. Highly Luminescent Linear Complex Arrays of up to Eight Cuprous Centers. *Chem. - Eur. J.* **2016**, *22*, 2396–2405.

(11) Stollenz, M.; Meyer, F. Mesitylcopper – A Powerful Tool in Synthetic Chemistry. *Organometallics* **2012**, *31*, 7708–7727.

(12) For synthetic and structural aspects of 1,3,5-triazapentadienes including their transition metal and luminescent BF₂/BPh₂ complexes, see: (a) Ley, H.; Müller, F. Über zwei neue Klassen Metallsalze bildender Imidbasen. Beitrag zur Theorie der inneren Metallkomplexsalze. Ber. Dtsch. Chem. Ges. 1907, 40, 2950-2958. (b) Cooper, F. C.; Partridge, M. W.; Short, W. F. 88. Diamidides. Part I. Derivatives of Triazapentadiene and Tetra-azaheptatriene. J. Chem. Soc. 1951, 391-404. (c) Peak, D. A. Diamides. Part II. 2:4-Diaryltriazapentadienes. J. Chem. Soc. 1952, 215-226. (d) Schulte, N.; Fröhlich, R.; Hecht, J.; Würthwein, E.-U. Synthesis, Structure, and Reactivity of Alkoxy-Substituted 2,4-Diazapentadienylium-, 2,4,6-Triazaheptatrienylium-, and 2,4,6,8-Tetraazanonatetraenylium Salts. Liebigs Ann. 1996, 371-380. (e) Heße, N.; Fröhlich, R.; Wibbeling, B.; Würthwein, E.-U. 1,3,5-Triazapenta-1,3-dienes: Useful Building Blocks for the Synthesis of 1,2-Dihydro-1,3,5-triazines and Oligonitriles. Eur. J. Org. Chem. 2006, 2006, 3923-3937. (f) Gilroy, J. B.; Ferguson, M. J.; McDonald, R.; Patrick, B. O.; Hicks, R. G. Formazans as β -diketiminate analogues. Structural characterization of boratatetrazines and their reduction to borataverdazyl radical anions. Chem. Commun. 2007, 126-128. (g) Marihart, E. A.; Greving, J.-B.; Fröhlich, R.; Würthwein, E.-U. (5-Imino-4,5-dihydro-3H-pyrrol-2yl)amines as Sterically Restrained 1,3,5-Triazapenta-1,3-dienes: Useful Building Blocks for the Synthesis of Oligonitriles. Eur. J. Org. Chem. 2007, 5071-5081. (h) Greving, J.-B.; Behrens, H.; Fröhlich, R.; Würthwein, E.-U. Multivalent 1-Oxa-3,5,7-triazahepta-1,3,5trienes: Synthesis, Structural Properties and Metal Coordination. Eur. J. Org. Chem. 2008, 5740-5754. (i) Häger, I.; Fröhlich, R.; Würthwein, E.-U. Synthesis of Secondary, Tertiary and Quaternary 1,3,5-Triazapenta-1,3-dienes and Their Co^{II}, Zn^{II}, Pd^{II}, Cu^{II} and BF₂ Coordination Compounds. Eur. J. Inorg. Chem. 2009, 2415-2428. (j) Clodt, J. I.; Wigbers, C.; Reiermann, R.; Fröhlich, R.; Würthwein, E.-U. Synthesis and Aggregation Properties of Two- and Three-Armed Nitrogen-Rich Chelate Ligands: Novel Bis(N-acylamidines), Tris(N-acylamidines) and Bis(triazapentadienes) with Flexible or Rigid Spacers. Eur. J. Org. Chem. 2011, 3197-3209. (k) Glotzbach, C.; Gödeke, N.; Fröhlich, R.; Daniliuc, C.-G.; Saito, S.; Yamaguchi, S.; Würthwein, E.-U. Fluorescent benzene-centered mono-, bis- and tristriazapentadiene-boron complexes. Dalton Trans. 2015, 44, 9659-9671

(13) For Group 1/2/13 and Group 7-12 metal complexes of 1,3,5triazapentadienyl anions, see refs 12h,i and (a) Siedle, A. R.; Webb, R. J.; Behr, F. E.; Newmark, R. A.; Weil, D. A.; Erickson, K.; Naujok, R.; Brostrom, M.; Mueller, M.; Chou, S.-H.; Young, V. G., Jr. Perfluoroalkyl-Substituted Triazapentadienes and Their Metal Complexes. Inorg. Chem. 2003, 42, 932-934. (b) Siedle, A. R.; Webb, R. J.; Brostrom, M.; Chou, S.-H.; Weil, D. A.; Newmark, R. A.; Behr, F. E.; Young, V. G., Jr. Reactions of the Perfluoroalkyltriazapentadiene $Ph_2N_3C_2(C_3F_7)_2H$ with Acids, Bases, and Water. Inorg. Chem. 2003, 42, 2596-2601. (c) Siedle, A. R.; Webb, R. J.; Brostrom, M.; Newmark, R. A.; Behr, F. E.; Young, V. G., Jr. Structure and Dynamics in a Bis(perfluoroalkyl)triazapentadiene Methylmercury Compound. Organometallics 2004, 23, 2281-2286. (d) Dias, H. V. R.; Singh, S. Copper(I) Complexes of Fluorinated Triazapentadienyl Ligands: Synthesis and Characterization of $[N\{(C_3F_7)C(Dipp)N\}_2]CuL$ (Where L = NCCH₃, CNBu^t, CO; Dipp = 2,6-Diisopropylphenyl). Inorg. Chem. 2004, 43, 5786-5788. (e) Dias, H. V. R.; Singh, S. Silver(I) Complexes of a Sterically Demanding Fluorinated Triazapentadienyl Ligand $[N\{(C_3F_7)C(Dipp)N\}_2]^-$ (Dipp = 2,6-Diisopropylphenyl). Inorg. Chem. 2004, 43, 7396-7402. (f) Dias, H. V. R.; Singh, S.; Cundari, T. R. Monomeric Thallium(I) Complexes of Fluorinated Triazapentadienyl Ligands. Angew. Chem., Int. Ed. 2005, 44, 4907-4910. (g) Dias, H. V. R.; Singh, S. Monomeric lithium triazapentadienyl complexes. Dalton Trans. 2006, 1995-2000. (h) Dias, H. V. R.; Singh, S.; Flores, J. A. Syntheses of Highly

Fluorinated 1,3,5-Triazapentadienyl Ligands and Their Use in the Isolation of Copper(I)-Carbonyl and Copper(I)-Ethylene Complexes. Inorg. Chem. 2006, 45, 8859-8861. (i) Flores, J. A.; Dias, H. V. R. Gold(I) Ethylene and Copper(I) Ethylene Complexes Supported by a Polyhalogenated Triazapentadienyl Ligand. Inorg. Chem. 2008, 47, 4448-4450. (j) Dias, H. V. R.; Flores, J. A.; Wu, J.; Kroll, P. Monomeric Copper(I), Silver(I), and Gold(I) Alkyne Complexes and the Coinage Metal Family Group Trends. J. Am. Chem. Soc. 2009, 131, 11249-11255. (k) Flores, J. A.; Badarinarayana, V.; Singh, S.; Lovely, C. J.; Dias, H. V. R. Synthesis and catalytic activity of an electron-deficient copper-ethylene triazapentadienyl complex. Dalton Trans. 2009, 7648-7652. (1) Dias, H. V. R.; Flores, J. A.; Pellei, M.; Morresi, B.; Lobbia, G. G.; Singh, S.; Kobayashi, Y.; Yousufuddin, M.; Santini, C. Silver(I) and copper(I) complexes supported by fully fluorinated 1,3,5-triazapentadienyl ligands. Dalton Trans. 2011, 40, 8569-8580. (m) Flores, J. A.; Kobayashi, Y.; Dias, H. V. R. Synthesis and characterization of silver(I) adducts supported solely by 1,3,5triazapentadienyl ligands or by triazapentadienyl and other N-donors. Dalton Trans. 2011, 40, 10351-10359. (n) Adiraju, V. A. K.; Flores, J. A.; Yousufuddin, M.; Dias, H. V. R. Copper(I) Ethylene Complexes Supported by 1,3,5-Triazapentadienyl Ligands with Electron-Withdrawing Groups. Organometallics 2012, 31, 7926-7932. (o) Pernik, I.; Maitland, B. J.; Stasch, A.; Jones, C. Synthesis and attempted reductions of bulky 1,3,5-triazapentadienyl groups 2 and 13 halide complexes. Can. J. Chem. 2018, 96, 513-521. (p) Singh, S.; Wang, G.; Mao, J. X.; Flores, J. A.; Kou, X.; Campana, C.; Kroll, P.; Dias, H. V. R. Gold(I) Complexes $[N\{(C_3F_7)C(Dipp)N\}_2]AuL$ (L = Ethylene, tert-Butyl Isocyanide, Tetrahydrothiophene, Triphenylphosphine) and Different Triazapentadienyl Ligand Coordination Modes. Eur. J. Inorg. Chem. 2016, 2016, 5435-5444. (q) Ponduru, T. T.; Qiu, C.; Mao, J. X.; Leghissa, A.; Smuts, J.; Schug, K. A.; Dias, H. V. R. Copper(I)based oxidation of polycyclic aromatic hydrocarbons and product elucidation using vacuum ultraviolet spectroscopy and theoretical spectral calculations. New J. Chem. 2018, 42, 19442-19449.

(14) For application as ligands in Zn(II)- and Al(III)-catalyzed transformations, see: (a) Bakthavachalam, K.; Reddy, N. D. Synthesis of Aluminum Complexes of Triaza Framework Ligands and Their Catalytic Activity toward Polymerization of ε -Caprolactone. *Organometallics* **2013**, *32*, 3174–3184. (b) Kulkarni, N. V.; Das, A.; Ridlen, S. G.; Maxfield, E.; Adiraju, V. A. K.; Yousufuddin, M.; Dias, H. V. R. Fluorinated triazapentadienyl ligand supported ethyl zinc(II) complexes: reaction with dioxygen and catalytic applications in the Tishchenko reaction. *Dalton Trans.* **2016**, *45*, 4896–4906. (c) Kirubakaran, B.; Beesam, R.; Reddy Nareddula, D. Zinc(II) complexes of Triaza and Amidinate ligands: Efficient initiators for the ring-opening polymerization of ε -Caprolactone and *rac*-Lactide. *Appl. Organomet. Chem.* **2017**, *31*, e3833.

(15) For metal complexes and salts of 1,5-diarylpentaazdienides, see: (a) Beck, J.; Strähle, J. Complexes of 1,5-Di(p-tolyl)-l,4-pentaazadien-3-ide, Crystal Structures of $[Cu(tolylNNNNNtolyl)]_3$ and INi(toIyINNNNNtolyl)2]2. Angew. Chem., Int. Ed. Engl. 1985, 24, 409-410. (b) Schmid, R.; Beck, J.; Strähle, J. Synthesis and Structure of Cesium 1,5-Bis(p-tolyl)pentaazadienide, Cs⁺(tolN₅tol)⁻. Z. Naturforsch., B: J. Chem. Sci. 1988, 43, 529-532. (c) Beck, J. Synthesis and Crystal Structure of (Cyclopentadienyl)(dicarbonyl)(l,5-di-p-tolylpentaazadienido)molybdenum, (Cp)Mo(CO)₂(tolN₅tol). Z. Naturforsch., B: J. Chem. Sci. 1988, 43, 1029-1032. (d) Beck, J. The Crystal Structures of (l,5-Ditolylpentaazadienido)(triphenylphosphane)gold-(I) and l,5-Ditolyl-3-methylpentaazadiene. Z. Naturforsch., B: J. Chem. Sci. 1988, 43, 1219-1223. (e) Schmid, R.; Strähle, J. Synthesis and Structure of Trimeric 1,5-Bis(p-ethoxyphenyl)pentaazadienidocopper(I) - A Complex with Short Cu-Cu Contacts in a Linear Cu₃³⁺ Unit. Z. Naturforsch., B: J. Chem. Sci. 1989, 44, 105–109. (f) Dieterich, S.; Strähle, J. The Structure of the Pentaazadienide Anion [tol-N=N-N-N=N-tol]. Synthesis and Crystal Structure of $Cs_2(18-Crown-6)(tolN_5tol)_2$ and $(NH_4)[Cr(NH_3)_6(H_2O)_4]_-$ (tolN₅tol)₄. Z. Naturforsch., B: J. Chem. Sci. **1993**, 48, 1574–1580. (g) Dieterich, S.; Strähle, J. Pentaazadienido complexes of zinc, cadmium, and mercury. The crystal structure of [Cd(EtOC₆H₄-N₅-

 $C_6H_4OEt)_2(py)_2$] and [Hg(tol-N₅-tol)₂(py)]. Z. Anorg. Allg. Chem. 1994, 620, 145–150.

- (16) (a) Oxley, P.; Short, W. F. Amidines. Part III. Preparation of Substituted Amidines from Ammonium or Substituted Ammonium Salts and N-Acylbenzenesulphonalkylamides or Acylbenzenesulphonalkylanilides. J. Chem. Soc. 1947, 382-389. (b) Oxley, P.; Short, W. F. Amidines. Part IX. Preparation of Substituted Amidines from Ketoxime Sulphonates and Ammonia or Amines. J. Chem. Soc. 1948, 1514-1527. (c) Cotton, F. A.; Lei, P.; Murillo, C. A.; Wang, L.-S. Synthesis of unsymmetrical formamidines and benzamidines: structural studies of copper, cobalt and chromium complexes. Inorg. Chim. Acta 2003, 349, 165-172. (d) Liu, F.-S.; Gao, H.-Y.; Song, K.-M.; Zhang, L.; Zhu, F.-M.; Wu, Q. Nickel complexes bearing [N,N] 2pyridylbenzamidine ligands: Syntheses, characterizations, and catalytic properties for ethylene oligomerization. Polyhedron 2009, 28, 1386-1392. (e) Huang, Y.-T.; Tang, X.; Yang, Y.; Shen, D.-S.; Tan, C.; Liu, F.-S. Efficient pyridylbenzamidine ligands for palladium-catalyzed Suzuki-Miyaura reaction. Appl. Organomet. Chem. 2012, 26, 701-706. (g) Niu, Y.-P.; Wang, X.-W.; Zheng, Z.-W.; Ma, X.-F.; Cai, J.-Q.; Zhang, J.-K.; Cheng, J.-L. Vinyl polymerization of norbornene catalyzed by 2-Py-amidine Ni(II) complex/methylaluminoxane systems. Appl. Organomet. Chem. 2014, 28, 688-695. (h) Tognon, A.; Rosar, V.; Demitri, N.; Montini, T.; Felluga, F.; Milani, B. Coordination chemistry to palladium(II) of pyridylbenzamidine ligands and the related reactivity with ethylene. Inorg. Chim. Acta 2015, 431, 206-218.
- (17) Loh, C.; Seupel, S.; Koch, A.; Görls, H.; Krieck, S.; Westerhausen, M. Strong intramolecular calcium— π interactions with aryl substituents requirements and limitations. *Dalton Trans.* **2014**, *43*, 14440—14449.
- (18) Due to the presence of dynamically interconverting (*syn/anti*) *EE, EZ/ZE,* and *ZZ* isomers, the ¹H and ¹³C{¹H} NMR spectra of **1** have not been reported as an even greater multiplicity of resonance signals was observed that could not be unambiguously assigned.
- (19) For previous reports about hydrogen bonds on correlations between ¹H NMR chemical shifts and crystallographic data, see: (a) Bertolasi, V.; Gilli, P.; Ferretti, V.; Gilli, G. Intramolecular O–H··· O hydrogen bonds assisted by resonance. Correlation between crystallographic data and ¹H NMR chemical shifts. *J. Chem. Soc., Perkin Trans.* 2 1997, 945–952. (b) Harris, T. K.; Zhao, Q.; Mildvan, A. S. NMR studies of strong hydrogen bonds in enzymes and in a model compound. *J. Mol. Struct.* 2000, 552, 97–109.
- (20) (a) Ruiz-Morales, Y.; Schreckenbach, G.; Ziegler, T. Calculation of ¹²⁵Te Chemical Shifts Using Gauge-Including Atomic Orbitals and Density Functional Theory. *J. Phys. Chem. A* **1997**, *101*, 4121–4127. (b) Vivas-Reyes, R.; De Proft, F.; Biesemans, M.; Willem, R.; Geerlings, P. DFT Calculations of ¹¹⁹Sn Chemical Shifts Using Gauge-Including Atomic Orbitals and Their Interpretation via Group Properties. *J. Phys. Chem. A* **2002**, *106*, 2753–2759. (c) Bayse, C. A. Considerations for Reliable Calculation of ⁷⁷Se Chemical Shifts. *J. Chem. Theory Comput.* **2005**, *1*, 1119–1127. (d) Bühl, M.; Wrackmeyer, B. Density-functional computation of ⁹³Nb NMR chemical shifts. *Magn. Reson. Chem.* **2010**, *48*, S61–S68. (e) Arras, A.; Eichele, K.; Maryasin, B.; Schubert, H.; Ochsenfeld, C.; Wesemann, L. Intermolecular ¹¹⁹Sn, ³¹P Through-Space Spin–Spin Coupling in a Solid Bivalent Tin Phosphido Complex. *Inorg. Chem.* **2016**, *55*, 4669–4675.
- (21) The N-H resonance of 6 is too broad to be detected at room temperature but narrows around and below -30 °C. Between -30 and -100 °C, a downfield shift of 0.84 ppm is observed.
- (22) There is no evidence for the corresponding *anti* rotational isomers in the solid-state structures of 1-6.
- (23) Structure of **6**: In the structure, * indicate atoms generated by the following symmetry operations: (') x + 1, y, -z + 1/2; (") x, y + 1, z; ("') x + 1, y + 1, -z + 1/2; ('''') x + 1, y + 2, -z + 1/2; (''''') x, y + 2, z (also compare Figure S8).
- (24) Jeffrey, G. A. An Introduction to Hydrogen Bonding; Oxford University Press: New York, 1997.

- (25) Allen, F. H.; Kennard, O.; Watson, D. G.; Brammer, L.; Orpen, A. G.; Taylor, R. Tables of bond lengths determined by *X*-ray and neutron diffraction. Part 1. Bond lengths in organic compounds. *J. Chem. Soc., Perkin Trans.* 2 **1987**, S1–S19.
- (26) Holata, J.; Schmidt, P.; Ševčík, S.; Štamberg, J. Model Compounds of Hydrophilic Gels. II. An Interpretation of the IR Spectra of Polymers by Means of Substituted Amides of Pivalic Acid. Collect. Czech. Chem. Commun. 1972, 37, 2009–2014.
- (27) (a) APEX2: Program for Data Collection on Area Detectors; BRUKER AXS, Inc., Madison, WI. (b) APEX3: Program for Data Collection on Area Detectors; BRUKER AXS Inc.: Madison, WI.
- (28) Sheldrick, G. M. SADABS: Program for Absorption Correction of Area Detector Frames; University of Göttingen: Göttingen, 2008.
- (29) Sheldrick, G. M. TWINABS: Program for Performing Absorption Corrections to X-ray Diffraction Patterns Collected from Non-Merohedrally Twinned and Multiple Crystals; University of Göttingen, Göttingen, 2013.
- (30) (a) Sheldrick, G. M. A short history of SHELX. Acta Crystallogr., Sect. A: Found. Crystallogr. 2008, A64, 112–122. (b) Sheldrick, G. M. Crystal structure refinement with SHELXL. Acta Crystallogr., Sect. C: Struct. Chem. 2015, C71, 3–8.
- (31) (a) Spek, A. L. *PLATON: A Multipurpose Crystallographic Tool*; Utrecht University, Utrecht, The Netherlands, 2008. (b) Spek, A. L. Single-crystal structure validation with the program *PLATON. J. Appl. Crystallogr.* **2003**, *36*, 7–13.
- (32) Frisch, M. J.; Trucks, G. W.; Schlegel, H. B.; Scuseria, G. E.; Robb, M. A.; Cheeseman, J. R.; Scalmani, G.; Barone, V.; Mennucci, B.; Petersson, G. A.; Nakatsuji, H.; Caricato, M.; Li, X.; Hratchian, H. P.; Izmaylov, A. F.; Bloino, J.; Zheng, G.; Sonnenberg, J. L.; Hada, M.; Ehara, M.; Toyota, K.; Fukuda, R.; Hasegawa, J.; Ishida, M.; Nakajima, T.; Honda, Y.; Kitao, O.; Nakai, H.; Vreven, T.; Montgomery, J. A., Jr.; Peralta, J. E.; Ogliaro, F.; Bearpark, M.; Heyd, J. J.; Brothers, E.; Kudin, K. N.; Staroverov, V. N.; Kobayashi, R.; Normand, J.; Raghavachari, K.; Rendell, A.; Burant, J. C.; Iyengar, S. S.; Tomasi, J.; Cossi, M.; Rega, N.; Millam, J. M.; Klene, M.; Knox, J. E.; Cross, J. B.; Bakken, V.; Adamo, C.; Jaramillo, J.; Gomperts, R.; Stratmann, R. E.; Yazyev, O.; Austin, A. J.; Cammi, R.; Pomelli, C.; Ochterski, J. W.; Martin, R. L.; Morokuma, K.; Zakrzewski, V. G.; Voth, G. A.; Salvador, P.; Dannenberg, J. J.; Dapprich, S.; Daniels, A. D.; Farkas, Ö.; Foresman, J. B.; Ortiz, J. V.; Cioslowski, J.; Fox, D. J. Gaussian 09, Revision D.01; Gaussian, Inc.: Wallingford, CT, 2009.
- (33) (a) Becke, A. D. Density-functional exchange-energy approximation with correct asymptotic behavior. *Phys. Rev. A: At., Mol., Opt. Phys.* **1988**, 38, 3098–3100. (b) Becke, A. D. Density-functional thermochemistry. III. The role of exact exchange. *J. Chem. Phys.* **1993**, 98, 5648–5652. (c) Lee, C.; Yang, W.; Parr, R. G. Development of the Colic-Salvetti correlation-energy formula into a functional of the electron density. *Phys. Rev. B: Condens. Matter Mater. Phys.* **1988**, 37, 785–789.
- (34) Pople basis set reference for "6-311G". Addition of "d" adds polarization functions of *d*-type, and "+" adds diffuse functions to heavy elements: (a) McLean, A. D.; Chandler, G. S. Contracted Gaussian basis sets for molecular calculations. I. Second row atoms, *Z* = 11–18. *J. Chem. Phys.* **1980**, 72, 5639–5648. (b) Krishnan, R.; Binkley, J. S.; Seeger, R.; Pople, J. A. Self-consistent molecular orbital methods. XX. A basis set for correlated wave functions. *J. Chem. Phys.* **1980**, 72, 650–654.
- (35) (a) Ahlrichs, R.; Bär, M.; Häser, M.; Horn, H.; Kölmel, C. Electronic Structure Calculations on Workstation Computers: The Program System TURBOMOLE. Chem. Phys. Lett. 1989, 162, 165–169. (b) Furche, F.; Ahlrichs, R.; Hättig, C.; Klopper, W.; Sierka, M.; Weigend, F. Turbomole. Wiley Interdiscip. Rev.: Comput. Mol. Sci. 2014, 4, 91–100. (c) TURBOMOLE V7.2 2017, A development of University of Karlsruhe and Forschungszentrum Karlsruhe GmbH, 1989–2007; TURBOMOLE GmbH, 2007. http://www.turbomole.com.
- (36) Yanai, T.; Tew, P. D.; Handy, N. C. A new hybrid exchange—correlation functional using the Coulomb-attenuating method (CAM-B3LYP). *Chem. Phys. Lett.* **2004**, 393, 51–57.

The Journal of Organic Chemistry

- (37) Perdew, J. P. Density-functional approximation for the correlation energy of the inhomogeneous electron gas. *Phys. Rev. B: Condens. Matter Mater. Phys.* **1986**, 33, 8822–8824.
- (38) (a) Eichkorn, K.; Treutler, O.; Öhm, H.; Häser, M.; Ahlrichs, R. Auxiliary basis sets to approximate Coulomb potentials. *Chem. Phys. Lett.* **1995**, 242, 652–660. (b) Eichkorn, K.; Weigend, F.; Treutler, O.; Ahlrichs, R. Auxiliary basis sets for main row atoms and transition metals and their use to approximate Coulomb potentials. *Theor. Chem. Acc.* **1997**, 97, 119–124. (c) Sierka, M.; Hogekamp, A.; Ahlrichs, R. Fast evaluation of the Coulomb potential for electron densities using multipole accelerated resolution of identity approximation. *J. Chem. Phys.* **2003**, 118, 9136–9148.
- (39) Schäfer, A.; Horn, H.; Ahlrichs, R. Fully optimized contracted Gaussian basis sets for atoms Li to Kr. *J. Chem. Phys.* **1992**, 97, 2571–2577
- (40) Weigend, F.; Ahlrichs, R. Balanced basis sets of split valence, triple zeta valence and quadruple zeta valence quality for H to Rn: Design and assessment of accuracy. *Phys. Chem. Chem. Phys.* **2005**, *7*, 3297–3305.

■ NOTE ADDED AFTER ASAP PUBLICATION

This paper was published ASAP on September 27, 2019. Due to a production error, Figures 2 and 3 and Scheme 2 were in incorrect positions. The corrected version was reposted on September 30, 2019.